NUCLEAR SCIENCE AND ENGINEERING: **109**, 341–349 (1991)

Fission Cross-Section Measurements of ^{247}Cm, ^{254}Es, and ^{250}Cf from 0.1 eV to 80 keV

Y. Danon, R. E. Slovacek, and R. C. Block
Rensselaer Polytechnic Institute, Department of Nuclear Engineering and Engineering Physics Gaerttner Linac Laboratory, Troy, New York 12180-3590

R. W. Lougheed and R. W. Hoff
Lawrence Livermore National Laboratory, P.O. Box 808, Livermore, California 94550

and

M. S. Moore
Los Alamos National Laboratory, P.O. Box 1663, Los Alamos, New Mexico 87451

Received September 21, 1990
Accepted June 4, 1991

Abstract – *The fission cross sections of ^{247}Cm, ^{254}Es, and ^{250}Cf are measured with the Rensselaer intense neutron spectrometer from 0.1 eV to 80 keV. The cross sections are normalized to the ^{235}U ENDF/B-V broadened cross section. Fission areas and resonance widths are determined for low-energy resonances in ^{247}Cm. The ^{254}Es and ^{250}Cf fission cross sections are the only reported measurements for these isotopes. The ^{254}Es isotope is the heaviest odd-odd isotope ever measured over this energy range. The thermal fission cross sections for ^{247}Cm, ^{254}Es, and ^{250}Cf are determined by extrapolation of the low-energy region of the cross section and are in good agreement with other reported measurements. Resonance integrals are reported for the energy range of 0.1 eV to 80 keV, and the areas for ^{247}Cm and ^{250}Cf resonances are also reported. The previously reported ^{246}Cm fission cross section was corrected for fission in ^{247}Cm.*

I. INTRODUCTION

The fission cross sections of the even curium isotopes ^{242}Cm, ^{244}Cm, ^{246}Cm, and ^{248}Cm were measured at Rensselaer Polytechnic Institute (RPI) previously by Maguire et al.[1] and Alam et al.[2] This measurement completes the fission cross-section measurement set for the curium isotopes.

Einsteinium-254 has a short half-life of 276 days and therefore has a high alpha-particle activity. The fission cross section of such a heavy odd-odd nucleus is interesting for its physical properties, and as is shown, the ^{254}Es fission cross section looks different from all other measurements and shows an interesting lack of structure.

The ^{250}Cf measurement was taken to correct for possible contamination in the einsteinium sample, which decays by alpha- and beta-particle emission to ^{250}Cf. Because of the high rate of spontaneous fission, this sample had the lowest signal-to-background ratio ever measured in the Rensselaer intense neutron spectrometer (RINS).

The einsteinium, curium, and californium isotopes that were measured are hard to obtain, and only microgram or submicrogram quantities of samples were available; however, the RINS system has the capability to measure such small samples because of its high neutron flux. The RINS system couples the RPI 60-MeV electron linear accelerator (linac) to a lead slowing-down-time spectrometer that consists of a helium-cooled tantalum target inside a 1.8 m on a side, 75-t lead cubic pile.[3] The RINS produces a very intense broad-resolution neutron flux in the energy range of 0.1 to 80000 eV. The flux intensity obtained is $\sim 10^4$

times greater than an equivalent resolution from a 5-m time-of-flight (TOF) experiment.[3] The RINS neutron density has a Gaussian shape with an energy resolution of ~0.35 [full-width at half-maximum (FWHM) $\Delta E/E$] from 1 eV to 1 keV.

In order to measure highly alpha-particle active samples, the hemispherical fission chamber was developed[4] and used in previous RPI RINS measurements of heavy transactinides.[1,2] The chamber's hemispherical shape combined with very fast rise time custom-designed electronics[5,6] reduces the alpha-particle pileup problem that might be troublesome otherwise.

II. EXPERIMENTAL METHOD

The RINS system provides an intense source of neutrons with an average neutron energy E (in electron-volts) given by[3]

$$E = \frac{165\,000}{(t + 0.3)^2} , \tag{1}$$

where t is the slowing-down time in microseconds. During the linac pulse, the electrons hit the tantalum target and produce intense bremsstrahlung radiation that in turn produces neutrons by a (γ,n) reaction. The pulse of bremsstrahlung, also called gamma flash, causes a high count rate in the fission chamber (due to gamma-induced ionization) and will show up in one of the early channels of the TOF spectrum; this channel is defined as slowing-down-time zero ($t = 0$). The lead slowing-down-time spectrometer resolution function was first derived theoretically by Bergman et al.[7] Fisher[8] made a Monte Carlo calculation with the MCNP code[9] and fitted his numerical resolution results to the Bergman et al. theoretical form. The resolution function used by Stopa[5] and Alam[6] was used in this work in a resolution-broadening program; the resolution function is given by

$$\left(\frac{dE}{E}\right)_{\text{FWHM}} = \left[0.0835 + \left(\frac{0.128}{E}\right) + 3.05 \times 10^{-5} E\right]^{1/2} . \tag{2}$$

The relative energy-dependent neutron flux was also fitted by Fisher[8] and is given by

$$\phi_r(E) = E^{-0.776} \exp\left[-\left(\frac{0.214}{E}\right)^{1/2}\right] , \tag{3}$$

where E represents the average neutron energy as given by Eq. (1). The hemispherical fission chamber used by Alam et al.[2] and Alam[6] was used in this experiment; the chamber was filled with 2 atm (absolute) of pure methane gas and was operated with a 500-V negative bias. The sample order in the chamber is shown in Fig. 1. The $^{235}U + ^{252}Cf$ and ^{252}Cf samples are the same samples used by Alam in his experiment. The ^{247}Cm, ^{250}Cf, and ^{254}Es samples were chemically purified to remove other actinides and any interfering nuclides prior to the measurement. The isotopic content of the samples is listed in Table I. The purified samples were then electroplated as ~6-mm-diam spots on the surfaces of hemispherical nickel foils that were assembled in the fission chamber. The electroplating solution was a mixture of 95% isopropyl alcohol and 5% 0.2 N

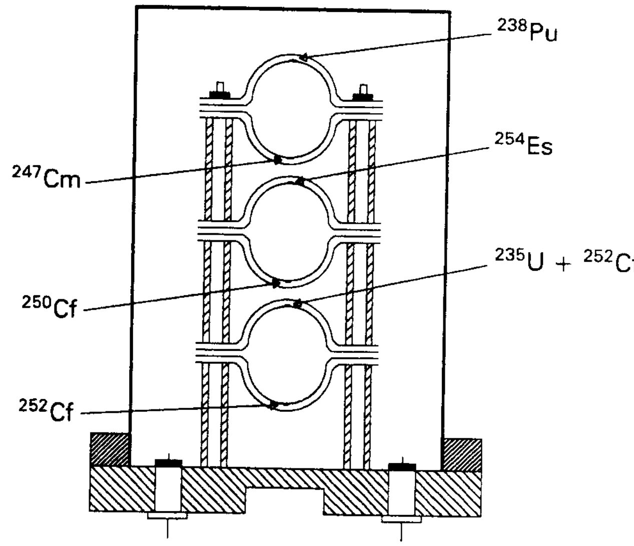

Fig. 1. A side-view sketch of the inside of the fission chamber (not to scale; see Ref. 2 for more details).

TABLE I

Sample Contents in the Fission Chamber

Sample	Content
^{252}Cf	313.5 ± 0.1 pg (212.01 ± 0.08 fission/s)[a]
$^{235}U + ^{252}Cf$	6.37 μg ^{235}U (0.619 ± 0.004 fission/s)[a]
^{250}Cf	0.149 ± 0.008 μg (441.87 ± 0.11 fission/s)[a]
^{254}Es	0.21 ± 0.01 μg [13.03 ± 0.02 fission/s (due to ^{250}Cf)][a]
^{247}Cm	3.16 ± 0.024 μg ^{247}Cm 3.48 μg ^{244}Cm 0.093 μg ^{245}Cm 3.96 μg ^{246}Cm 0.003 μg ^{240}Pu (30.86 ± 0.03 fission/s)[a]

[a]The spontaneous fission count rate of the sample.

HCI. To minimize ^{250}Cf contamination in the einsteinium sample, the ^{250}Cf was separated from the ^{254}Es at Lawrence Livermore National Laboratory (LLNL) 48 h before beginning the collection of data at RPI. The ^{247}Cm is from the same sample used by Moore and Keyworth[10] in their experiment in 1969. The mass content of the ^{247}Cm sample was corrected for isotopic decay. The sample contents are listed in Table I.

Each fission chamber is connected in sequence to a fast preamplifier, a power filter module [both custom designed by Oak Ridge National Laboratory (ORNL) (Ref. 2)], a LeCroy 612M amplifier, and a constant fraction discriminator ORTEC 473A. The constant fraction discriminator was set to a 1.5-V integral discrimination level to discriminate against the lower amplitude alpha-particle signals and electronic noise. The fission detection efficiency was determined by recording the spontaneous fission count rate as a function of discrimination level and by fitting the plateau region to an exponential. The ratio of the count rate at a 1.5-V discrimination level to the extrapolated count rate at zero discrimination is the efficiency η for that sample. The output from each constant fraction discriminator was connected to a TOF clock and an HP-1000, A-900 computer for the data acquisition.

The cylindrical fission chamber was inserted 90 cm deep into the 75-t lead pile in a hole whose axis is 60 cm from the bottom and rear face of the lead cube and was surrounded by machined lead blocks so that there were no big air gaps between the chamber and the lead. The RPI linac was operated at an average current of 15 μA and an average pulse rate of 90 pulse/s, which gave an average power of 900 W on the tantalum target. The linac pulse width was 200 ns. Data were taken for ~29 h with the linac on and 8 h with the linac off to measure the spontaneous fission background.

III. EXPERIMENTAL DATA REDUCTION

The data were collected in 29 separate files with each file representing a sum of ~1 h of data collecting. The first step was to correct each run for dead time and sum all runs to get one file that contained all the raw data. Since the resolution of the lead spectrometer is relatively broad, the second step was grouping the data into macrochannels with wider time widths than the basic clock channels. The grouping was done in a consistent way with the RINS resolution so that the energy width of the macrochannels did not exceed 25% of the RINS resolution width. The data were reduced from 3072 channels to 150 macrochannels, which gave an improvement of the counting statistics per channel.

The counts in channel i for sample x can be calculated by the following equation:

$$C_i^x = F \cdot \eta^x N^x \phi_r(E_i) \bar{\sigma}_f^x(E_i) \Delta E_i \ , \tag{4}$$

where

C_i^x = counts from sample x in macrochannel i

F = flux normalization factor

η^x = fission detection efficiency

N^x = number of atoms of sample x

E_i = average energy of macrochannel i

$\phi_r(E_i)$ = relative energy-dependent flux given by Eq. (3)

$\bar{\sigma}_f^x(E_i)$ = resolution-broadened fission cross section of sample x in channel i

ΔE_i = channel i width in energy units ($\Delta E_i = E_{i+1} - E_i$).

The third step was to find the flux normalization factor relative to ^{235}U. This was done by first taking the ENDF/B-V (Ref. 11) point cross-section file for ^{235}U and broadening the cross section with the RINS resolution, ending up with a broadening cross section at average macrochannel energies. The normalization factor is calculated by

$$F = \frac{C_i^{235}}{\eta^{235} N^{235} \phi_r(E_i) \bar{\sigma}_f^{235}(E_i) \Delta E_i} \ . \tag{5}$$

The term $\bar{\sigma}_f(E_i)$ is the ^{235}U broadened fission cross section given by

$$\bar{\sigma}_f(E_i) = \frac{1}{\sqrt{E_i}} \int_{E_{min}}^{E_{max}} G(E, E_i) \sqrt{E} \sigma_f(E) \, dE \ , \tag{6}$$

where

$\sigma_f(E)$ = ENDF/B-V (Ref. 11) ^{235}U fission cross section

$G(E, E_i)$ = Gaussian resolution function[6] of the RINS system around energy E_i.

Equation (5) was applied to each channel corresponding to neutron energies from 0.7 to 50 keV. The channel normalization factors were then averaged to give the overall normalization factor F. The standard deviation of the average was taken as the error in F, and this error is 4% over the above normalization energy range. A normalization over all the RINS energy range from 0.1 eV to 100 keV gave a normalization factor that is 5% smaller than the normalization factor used, and this is not a large discrepancy relative to the 10% overall error in the cross section obtained. After F was obtained, the fission cross section of sample x at macrochannel i is given simply by

$$\sigma_f(E_i) = \frac{1}{\eta^x N^x} \frac{C_i^x}{F \phi_r(E_i) \Delta E_i} \ . \tag{7}$$

TABLE II

Fission Cross Sections and 1σ Error*

Energy (eV)	^{247}Cm σ_f (b)	^{254}Es σ_f (b)	^{250}Cf σ_f (b)	Energy (eV)	^{247}Cm σ_f (b)	^{254}Es σ_f (b)	^{250}Cf σ_f (b)	Energy (eV)	^{247}Cm σ_f (b)	^{254}Es σ_f (b)	^{250}Cf σ_f (b)
0.116E+00[a]	56(6)	755(70)	−60(92)	0.192E+02	63(7)	82(8)	3(5)	0.381E+03	16(2)	22(2)	0(1)
0.150E+00	50(6)	698(65)	7(73)	0.205E+02	51(6)	79(7)	9(5)	0.410E+03	15(2)	21(2)	2(1)
0.189E+00	45(5)	621(58)	−22(61)	0.220E+02	40(5)	79(7)	2(4)	0.443E+03	15(2)	20(2)	−0.4(0.9)
0.233E+00	41(5)	574(53)	−5(52)	0.236E+02	33(4)	77(7)	4(4)	0.473E+03	15(2)	18(2)	1(1)
0.282E+00	39(4)	528(49)	77(46)	0.254E+02	28(3)	77(7)	1(4)	0.499E+03	15(2)	17(2)	1(1)
0.336E+00	36(4)	495(46)	76(41)	0.270E+02	26(3)	74(7)	3(5)	0.528E+03	15(2)	18(2)	0(1)
0.396E+00	36(4)	449(42)	111(38)	0.284E+02	26(3)	71(7)	5(4)	0.559E+03	14(2)	16(2)	0.0(0.9)
0.461E+00	36(4)	430(40)	169(37)	0.300E+02	25(3)	67(6)	9(4)	0.593E+03	14(2)	16(2)	0.5(0.9)
0.532E+00	38(4)	406(38)	184(35)	0.317E+02	25(3)	67(6)	6(4)	0.631E+03	13(1)	16(2)	1.1(0.9)
0.611E+00	47(5)	389(36)	162(32)	0.335E+02	25(3)	62(6)	1(4)	0.672E+03	13(1)	16(2)	1.4(0.8)
0.697E+00	74(8)	350(32)	110(28)	0.355E+02	25(3)	64(6)	3(4)	0.717E+03	12(1)	15(1)	0.4(0.8)
0.789E+00	146(16)	344(32)	99(26)	0.377E+02	26(3)	64(6)	9(4)	0.766E+03	12(1)	15(1)	0.8(0.8)
0.890E+00	285(31)	325(30)	43(23)	0.401E+02	28(3)	61(6)	4(3)	0.821E+03	11(1)	15(1)	0.3(0.7)
0.998E+00	472(51)	314(29)	18(21)	0.427E+02	32(4)	57(5)	3(3)	0.882E+03	11(1)	14(1)	0.1(0.7)
0.112E+01	625(68)	288(27)	30(20)	0.456E+02	36(4)	59(6)	2(3)	0.951E+03	10(1)	13(1)	0.7(0.6)
0.124E+01	647(70)	269(25)	44(19)	0.488E+02	41(5)	58(5)	5(3)	0.103E+04	10(1)	13(1)	0.9(0.6)
0.138E+01	539(58)	253(23)	2(18)	0.523E+02	45(5)	57(5)	4(3)	0.111E+04	9(1)	13(1)	0.6(0.6)
0.152E+01	383(41)	240(22)	13(17)	0.562E+02	50(6)	57(5)	2(3)	0.121E+04	9(1)	12(1)	0.6(0.5)
0.168E+01	259(28)	229(21)	27(16)	0.595E+02	53(6)	56(5)	5(4)	0.129E+04	9(1)	11(1)	−0.3(0.7)
0.184E+01	181(20)	216(20)	−12(15)	0.618E+02	56(6)	55(5)	2(3)	0.137E+04	8.4(0.9)	11(1)	−0.1(0.5)
0.202E+01	147(16)	202(19)	10(15)	0.643E+02	57(6)	51(5)	5(3)	0.149E+04	8.1(0.9)	12(1)	0(0)
0.221E+01	149(16)	194(18)	20(14)	0.669E+02	59(7)	52(5)	4(3)	0.162E+04	8.0(0.9)	10(1)	−0.5(0.5)
0.242E+01	191(21)	186(17)	6(13)	0.696E+02	59(7)	51(5)	2(3)	0.177E+04	7.8(0.9)	11(1)	−0.4(0.4)
0.265E+01	258(28)	175(16)	0(13)	0.726E+02	58(6)	52(5)	6(3)	0.193E+04	7.8(0.9)	10.0(0.9)	−0.4(0.4)
0.288E+01	317(34)	167(16)	28(13)	0.757E+02	55(6)	49(5)	3(3)	0.210E+04	7.6(0.9)	9.4(0.9)	0.0(0.4)
0.314E+01	331(36)	156(15)	−3(11)	0.791E+02	50(6)	47(4)	−1(3)	0.229E+04	7.2(0.8)	9.3(0.9)	−0.1(0.4)
0.342E+01	297(32)	149(14)	4(11)	0.827E+02	46(5)	46(4)	1(3)	0.251E+04	6.9(0.8)	8.9(0.8)	0.0(0.4)
0.372E+01	257(28)	143(13)	8(10)	0.865E+02	41(5)	42(4)	0(3)	0.276E+04	6.6(0.7)	8.5(0.8)	−0.4(0.3)
0.404E+01	246(27)	136(13)	5(10)	0.906E+02	37(4)	42(4)	1(3)	0.304E+04	6.2(0.7)	8.5(0.8)	−0.2(0.3)
0.438E+01	248(27)	136(13)	−12(10)	0.956E+02	34(4)	40(4)	2(2)	0.338E+04	5.9(0.7)	8.0(0.8)	0.4(0.3)
0.473E+01	235(26)	136(13)	10(10)	0.102E+03	32(4)	38(4)	0(2)	0.374E+04	5.7(0.6)	8.2(0.8)	−0.1(0.3)
0.511E+01	203(22)	129(12)	8(9)	0.108E+03	29(3)	38(4)	0(2)	0.412E+04	5.5(0.6)	7.5(0.7)	−0.2(0.3)
0.553E+01	162(18)	128(12)	2(8)	0.115E+03	27(3)	38(4)	1(2)	0.455E+04	5.2(0.6)	7.2(0.7)	0.0(0.3)
0.598E+01	133(15)	127(12)	9(9)	0.124E+03	25(3)	37(3)	2(2)	0.507E+04	5.0(0.6)	6.7(0.6)	0.1(0.2)
0.643E+01	118(13)	121(11)	7(8)	0.132E+03	23(3)	36(3)	−2(2)	0.567E+04	4.7(0.5)	6.5(0.6)	0.1(0.2)
0.694E+01	108(12)	114(11)	−2(8)	0.142E+03	23(3)	34(3)	0(2)	0.639E+04	4.5(0.5)	6.2(0.6)	−0.1(0.2)
0.746E+01	100(12)	112(10)	7(8)	0.152E+03	23(3)	34(3)	1(2)	0.726E+04	4.2(0.5)	5.8(0.5)	−0.1(0.2)
0.799E+01	95(11)	106(10)	7(7)	0.162E+03	24(3)	32(3)	1(2)	0.831E+04	4.0(0.5)	5.8(0.5)	0.1(0.2)
0.858E+01	92(10)	98(9)	2(7)	0.173E+03	25(3)	30(3)	1(2)	0.961E+04	3.7(0.4)	5.4(0.5)	0.00(0.10)
0.923E+01	88(10)	91(9)	8(7)	0.184E+03	24(3)	29(3)	2(2)	0.112E+05	3.6(0.4)	5.1(0.5)	−0.10(0.10)
0.997E+01	79(9)	87(8)	3(6)	0.197E+03	24(3)	28(3)	3(1)	0.131E+05	3.4(0.4)	4.7(0.4)	0.00(0.10)
0.107E+02	69(8)	85(8)	7(7)	0.212E+03	23(3)	28(3)	2(1)	0.152E+05	3.2(0.4)	4.5(0.4)	0.00(0.10)
0.114E+02	58(6)	89(8)	−2(6)	0.228E+03	23(3)	27(3)	1(1)	0.177E+05	3.0(0.3)	4.4(0.4)	0(0)
0.122E+02	49(5)	90(8)	3(6)	0.243E+03	23(3)	26(2)	0(1)	0.210E+05	3.0(0.3)	4.2(0.4)	−0.08(0.09)
0.131E+02	43(5)	92(9)	10(6)	0.258E+03	22(2)	26(2)	0(1)	0.254E+05	2.8(0.3)	4.0(0.4)	−0.04(0.08)
0.141E+02	43(5)	88(8)	7(5)	0.274E+03	20(2)	26(2)	2(1)	0.312E+05	2.7(0.3)	3.8(0.4)	0.08(0.07)
0.151E+02	50(6)	92(9)	10(6)	0.291E+03	19(2)	24(2)	1(1)	0.393E+05	2.5(0.3)	3.7(0.3)	0.05(0.06)
0.160E+02	59(7)	90(8)	−2(6)	0.311E+03	18(2)	24(2)	2(1)	0.509E+05	2.4(0.3)	3.4(0.3)	0.01(0.05)
0.169E+02	67(8)	90(8)	5(5)	0.332E+03	17(2)	23(2)	0(1)	0.687E+05	2.3(0.3)	3.2(0.3)	0.00(0.04)
0.180E+02	69(8)	87(8)	3(5)	0.355E+03	16(2)	23(2)	0(1)	0.976E+05	2.0(0.2)	3.2(0.3)	−0.04(0.03)

*The 1σ error is in parentheses.
[a]Read as 0.116×10^0.

IV. RESULTS

The fission cross-section results for ^{247}Cm, ^{254}Es, and ^{250}Cf are listed in Table II and plotted in Figs. 2, 3, and 4. The errors shown in Table II and on Figs. 2, 3, and 4 are due to uncertainties in the fission counting efficiency, the number of atoms in the sample, the neutron flux normalization factor, and the counting statistics. We are able to observe resolved resonances and clusters of resonances below ~200 eV in the ^{247}Cm. At higher energies, the RINS resolution can no longer resolve resonances, and the observed fission cross section is smooth.

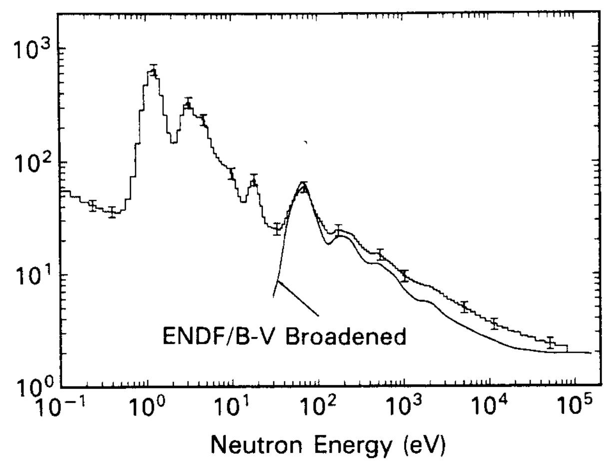

Fig. 2. The ^{247}Cm fission cross section.

IV.A. Curium-247

The ^{247}Cm sample was prepared from the same materials used in Moore and Keyworth's experiment,[10] and this sample contained impurities of mainly ^{244}Cm and ^{246}Cm, as shown in Table I. The fission cross section was corrected for these two isotopes using the results of previous measurements done at RPI by Stopa.[5] The correction was small (<1%) because of the high cross section of ^{247}Cm, relative to ^{244}Cm and ^{246}Cm. In this sample, resonances or clusters of partially resolved resonances were observed up to ~200 eV. The ^{247}Cm cross section reaches a peak of 647 b at 1.2 eV, and resonances were observed at 1.2, 3.1, 4.4, 9.2, and 18.0 eV. At these energies, the only other experimental results available are from the transmission measurement by Belanova et al.[12] They observed five resonances in their data at 1.247, 2.919, 3.189, 9.55, and 18.1 eV. Except for the 4.4-eV resonance, our resonance energies are in good agreement with their energies. The RINS system, however, could not resolve the resonances reported by Belanova et al. at 2.919 and 3.189 eV; we observed only one resonance at 3.1 eV. A resonance was observed at 4.4 eV that was not reported by Belanova et al., and it is possible that this resonance was lost in the corrections that they made for other curium, americium, and plutonium isotopes contained in their sample.

To determine the fission widths of the resonances observed, the area under each resonance was determined. The relation between the area under the resonance and the fission width is determined from the Breit-Wigner single-level formula:

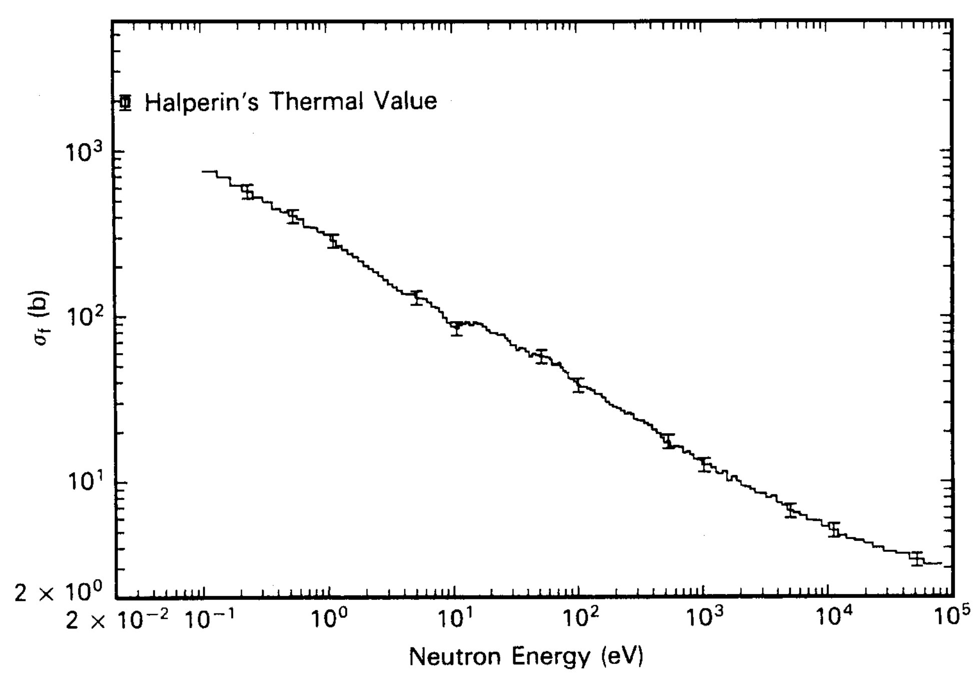

Fig. 3. The ^{254}Es fission cross section.

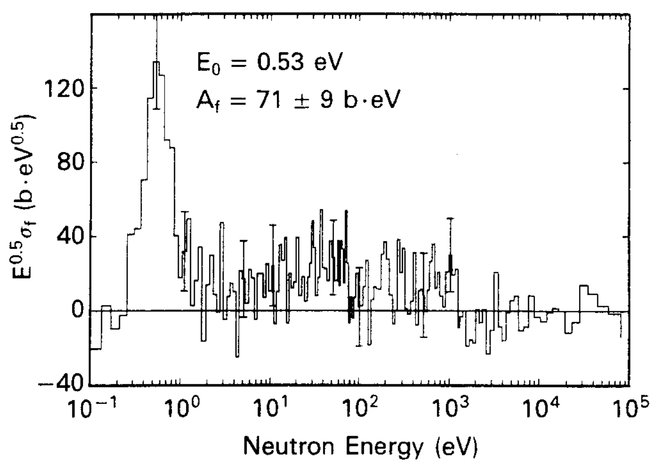

Fig. 4. The ^{250}Cf fission cross section.

$$A_f = \frac{\pi}{2} \sigma_0 \Gamma_f \ , \tag{8}$$

where

A_f = area under the resonance,

$$A_f = \sum \bar{\sigma}(E_i)\Delta E_i$$

$\bar{\sigma}(E_i)$ = fission cross section in barns at average energy of macrochannel i

σ_0 = peak cross section in barns given by

$$\sigma_0 = 1.302 \times 10^6 \frac{2g\Gamma_n(E_0)}{E_0\Gamma} \ , \tag{9}$$

where

E_0 = resonance peak energy (eV)

g = statistical weight factor for s-wave neutrons given by

$$g = \frac{2J+1}{2(2I+1)} \ ,$$

where

I = spin of the nucleus

$I = 9/2$ for ^{247}Cm and therefore $J = 4,5$ and $g = 0.5 \pm 0.05$

$\Gamma, \Gamma_n, \Gamma_f$ = total, neutron, and fission widths, respectively (eV).

The fission widths were calculated using Eq. (8) with the Γ and $2g\Gamma_n$ resonance parameters reported by Belanova et al.[12] Our results are reported in Table III, where the 1σ errors are due to errors in $\Gamma, 2g\Gamma_n$ reported by Belanova et al., and the error in calculating A_f. The errors in the resonance area A_f were calculated from the overall error in the fission cross section, as reported in Table II. The fission widths of ^{247}Cm were also estimated[13] by assuming $\Gamma_\gamma = 40$ meV and then $\Gamma_f(E) = \Gamma(E) - \Gamma_n(E) - \Gamma_\gamma(E)$; these results are also listed in Table III. A comparison of the two values shows very good agreement; the errors in the fission widths reported are mainly due to errors in the total width Γ as reported by Belanova et al.

Moore and Keyworth[10] measured the ^{247}Cm fission cross section directly by a nuclear explosion experiment, and their results are reported only for energies >20 eV; the resolution of their experiment is much better than the RINS resolution. The Moore and Keyworth fission cross section was broadened to the RINS resolution and plotted in Fig. 2. It is seen that both experiments agree on the shape of the cross section, but the Moore and Keyworth cross section is ~30% lower above 150 eV; the source of this discrepancy is unknown.

The fission cross-section low-energy tail was extrapolated to 0.025 eV, and a thermal fission of 106 ± 53 b was obtained for ^{247}Cm. This value agrees with

TABLE III

Resonance Parameters for ^{247}Cm in the Energy Range from 0.1 to 18.1 eV

Belanova et al.[12,a,b]			Mughabghab[13,c]	This Experiment[b]		
E (eV)	Γ (meV)	$2g\Gamma_n$ (meV)	Γ_f (meV)	Γ_f (meV)	A_f (b·eV)	E (eV)
1.247	74 ± 4	0.56 ± 0.09	34 ± 7	34 ± 6	427 ± 24	1.2
2.919	70 ± 30	0.1 ± 0.04	30 ± 30	---	---	---
3.189	130 ± 6	1.0 ± 0.1	62 ± 6	70 ± 14	444 ± 70	3.1
---	---	---	---	---	107 ± 47	4.4
9.55	166 ± 60	0.9 ± 0.33	125 ± 60	117 ± 83	141 ± 70	9.2
18.1	210 ± 170	3.7 ± 1.5	167 ± 170	166 ± 152	332 ± 46	18.0

[a]Resonance at 4.4 eV was not observed by Belanova et al.

[b]Resonances reported by Belanova et al. at 2.919 and 3.189 eV, observed in our experiment only as one resonance at 3.1 eV.

[c]Mughabghab[13] assumes $\Gamma_\gamma = 40$ meV and using Γ and Γ_n calculates Γ_f.

the Mughabghab-evaluated value[13] of 81.9 ± 4.1 b. The resonance integral from 0.1 eV to 80 keV was also calculated and found to be I_f = 890 ± 53 b, which is slightly higher than the evaluated value[13] of 760 ± 50 b. Other experimental results are presented in Table IV. The 6% error in the resonance integral is mainly the result of uncertainties in flux normalization, counting efficiency, and sample mass.

The ^{246}Cm fission cross section reported by Maguire et al.[1] has a resonance at 1.2 eV that was tentatively assigned to ^{246}Cm. Using the ^{247}Cm fission cross section measured in this experiment, we corrected the Maguire et al. measurement for the 0.084% ^{247}Cm impurity in their ^{246}Cm sample. The results of this correction are shown in Fig. 5, where it is seen that the 1.2-eV resonance that appeared in the ^{246}Cm measurement came from the 648-b resonance at 1.2 eV in ^{247}Cm.

The other fission cross sections of even curium isotopes measured at RPI previously[1,2] did not have any significant correction because of ^{247}Cm impurities in their samples.

IV.B. Einsteinium-254

The ^{254}Es sample is a pure sample with contamination only from the decay daughters of ^{254}Es, that is, ^{250}Bk and ^{250}Cf. The ^{250}Bk content in the sample is constant and was calculated to be ~0.04 wt%, which would have negligible effects on the fission cross section of ^{254}Es. The ^{250}Cf was growing into the sample during the measurement. When the experiment started ~48 h after the separation of ^{250}Cf and ^{250}Bk from the ^{254}Es at LLNL, we measured, by counting the spontaneous fission background, ~1 wt% of ^{250}Cf in the sample. At the end of the experiment, ~81 h later, we measured 2 wt% of ^{250}Cf in the sample. The effect of this ^{250}Cf buildup on the cross section is negligible because of the very low fission cross section of ^{250}Cf. The spontaneous fission of the ^{250}Cf was subtracted as a constant background counting rate.

The ^{254}Es fission cross section plotted in Fig. 3 shows very unusual structure. The cross section is decreasing as a function of energy in a rather smooth way with only some structure observed around 4.3 and 13.1 eV; the cross section seems to behave like $1/v$ up to 10 eV, and above 10 eV, it is falling slower than $1/v$. There are two possible explanations for not observing any structure in our measurement. As an odd-odd nucleus, the level spacing of ^{254}Es was calculated by Diamond et al.[15] using the Gilbert and Cameron[23] approach to be 1.1 eV. We calculated a level spacing of 0.9 eV using the Gilbert and Cameron approach assuming a binding energy of 6.26 MeV (calculated from the mass of ^{254}Es, ^{255}Es, and the neutron mass), a deformed nucleus model, and calculating the rest of the parameters (a and σ) from data given by Gilbert and Cameron; it is possible that the level spacing is even

TABLE IV

Thermal Fission Cross Section and Resonance Integrals* for ^{254}Es, ^{247}Cm, and ^{250}Cf

Sample	References	σ_f (0.025 eV) (b)	I_f (b)
^{254}Es	Diamond et al.[15]	3060 ± 180	---
	MacMurdo and Harbour[16]	2930 ± 130	2200 ± 90
	Halperin et al.[17]	1970 ± 200	1200 ± 250
	This Experiment	**1749 ± 110**	**896 ± 54**
^{247}Cm	Ice[18]	1400	---
	Diamond et al.[15]	108 ± 5	---
	Smith et al.[19]	409	---
	Halperin, Oliver, and Stoughton[20]	120 ± 12	1060 ± 110
	Benjamin, MacMurdo, and Spencer[14]	82 ± 5	778 ± 50
	Zhuravlev, Kroshkin, and Chetreikov[21]	80 ± 7	730 ± 70
	This Experiment	**106 ± 53**	**890 ± 53**
^{250}Cf	Metta et al.[22]	<350	---
	This Experiment	**112 ± 99**	**161 ± 39**

*The resonance integral is calculated as

$$I_f = \int_{0.5\ \mathrm{eV}}^{80\ \mathrm{keV}} \sigma(E)\frac{dE}{E} \ ;$$

the resonance integral for ^{250}Cf was calculated as

$$I_f = \int_{0.1\ \mathrm{eV}}^{80\ \mathrm{keV}} \sigma(E)\frac{dE}{E} \ .$$

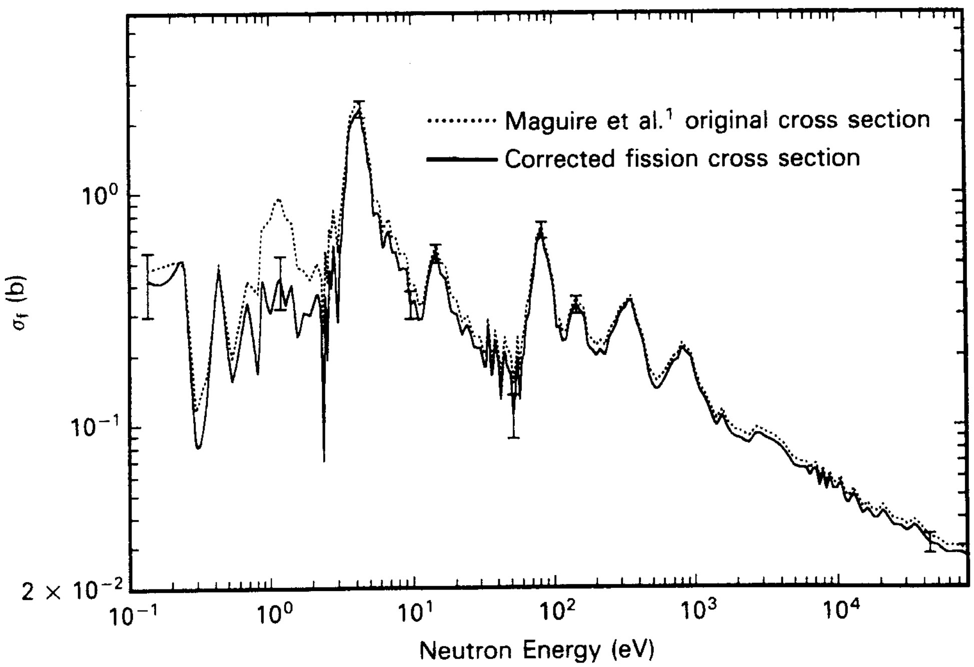

Fig. 5. The ^{246}Cm fission cross section corrected for ^{247}Cm impurities.

smaller than that which we calculated. With a small level spacing and no resonances below ~2 eV, the RINS system will not resolve any resonances, and all we could expect to see is a smooth cross section with some small wiggles due to structure. The other possibility is that ^{254}Es has large fission widths, larger than the level spacing; therefore, resonances overlap each other, and the continuum we see is the true structure of the ^{254}Es fission cross section. The answer to this problem can be found only by performing another experiment with better resolution.

The ^{254}Es fission cross section was extrapolated to 0.025 eV, and the thermal cross section was found to be 1749 ± 110 b. Table IV lists some other values of thermal cross sections for ^{254}Es. Our value is in good agreement with the Halperin et al.[17] value of 1970 ± 200 b. Our resonance integral was found to be 896 ± 54 b, which is lower than the Halperin et al. value of 1200 ± 250 and lower than MacMurdo and Harbour,[16] who measured 2200 ± 90. The 6% error in the resonance integral is mainly the result of uncertainties in flux normalization, counting efficiency, and sample mass.

IV.C. Californium-250

The ^{250}Cf sample was the smallest sample we had in this experiment, only 0.149 ± 0.008 μg. This sample also had the highest spontaneous fission rate of 442 ± 11 spontaneous fission/s. The signal-to-background ratio is very close to zero in most energy regions, but still we were able to see a single resolved resonance at 0.53 eV with a peak cross section of 184 ± 35 b and an area of 71 ± 9 b·eV and some structure in the energy range of 17 to 76 eV with an average cross section of ~4 b. The cross section multiplied by $\sqrt{E}$ is plotted in Fig. 4 and given in Table II. This result shows the advantage of using a lead slowing-down-time spectrometer to obtain high flux for such measurements. The fission cross section of ^{250}Cf was averaged in the energy range from 1.5 to 61 eV, and assuming a $1/v$ cross section, we extrapolated to 0.025 eV and calculated a contribution to the thermal cross section of 112 ± 99 b. We found only one other measurement by Metta et al.[22] that reported the cross section to be <350 b.

V. CONCLUSIONS

The fission cross sections of ^{254}Es and ^{250}Cf were first measured in the energy range of 0.1 eV to 80 keV. Einsteinium-254 showed only very little structure possibly because of wide fission widths and small level spacing; only further experiments with better resolution can verify that. The ^{250}Cf fission cross section has only one resonance at 0.53 eV and has an average cross section of the order of ~4 b in the 17- to 76-eV energy range.

This is the first ^{247}Cm fission cross-section measurement at the energy range of 0.1 to 20 eV, and the resonance parameters obtained are in good agreement with those from the Belanova et al. transmission measurement and Mughabghab's evaluation. In the energy range from 20 eV to 100 keV, the shape of the cross section agrees with the fission cross section measured by Moore and Keyworth, but >150 eV, our results are ~30% higher. Thermal cross sections were extrapolated for ^{254}Es and ^{247}Cm, and they are in good agreement with other experimental results; in the case of the ^{250}Cf thermal cross section, there is no other measurement with which to compare.

ACKNOWLEDGMENTS

The authors thank the members of the RPI linac operations staff for their friendly cooperation throughout the hours of data collection.

The authors are also indebted for the use of these rare isotopes to the Office of Basic Energy Science, U.S. Department of Energy (DOE) through the transplutonium element production facilities at ORNL. This work was performed under the auspices of DOE by the Division of Nuclear Physics under grant DE-FG02-88ER40475 and by LLNL under contract W-7405-ENG-48.

REFERENCES

1. H. T. MAGUIRE, C. R. S. STOPA, R. C. BLOCK, D. R. HARRIS, R. E. SLOVACEK, J. W. T. DABBS, R. J. DOUGAN, R. W. HOFF, and R. W. LOUGHEED, *Nucl. Sci. Eng.*, **89**, 293 (1985).

2. B. ALAM, R. C. BLOCK, R. E. SLOVACEK, and R. W. HOFF, *Nucl. Sci. Eng.*, **99**, 267 (1988).

3. R. E. SLOVACEK, D. S. CRAMER, E. B. BEAN, J. R. VALENTINE, R. W. HOCKENBURY, and R. C. BLOCK, *Nucl. Sci. Eng.*, **62**, 455 (1977).

4. J. W. T. DABBS, N. W. HILL, C. E. BEMIS, and S. RAMAN, "Fission Cross Section Measurements on Short-Lived Alpha Emitters," *Proc. Conf. Nuclear Cross Section Technology*, Washington, D.C., March 3–7, 1975, Special Publication 425, Vol. 1, p. 81, National Bureau of Standards (1975).

5. C. R. S. STOPA, "Measurements of Neutron Induced Fission Cross Sections of ^{244}Cm, ^{246}Cm, and ^{248}Cm by Means of Lead-Slowing-Down-Time," PhD Thesis, Rensselaer Polytechnic Institute (1983).

6. B. ALAM, "Measurements of the Neutron-Induced Fission Cross Sections of ^{242}Cm and ^{238}Pu by Lead Slowing Down Time," PhD Thesis, Rensselaer Polytechnic Institute (1987).

7. A. A. BERGMAN, A. I. ISACOFF, I. D. MURIN, F. L. SHAPIRO, I. V. SHTRANIKH, and M. V. CAZARNOVSKY, "A Neutron Spectrometer Based on Measuring the Slowing-Down Time of Neutrons in Lead," *Proc. 1st Int. Conf. Peaceful Uses Atomic Energy*, Geneva, August 8–20, 1955, United Nations, New York (1955).

8. H. M. FISHER, "Monte Carlo Feasibility Assessment of the Lead Slowing-Down Time Spectrometer for Spent Fuel Assay and Fuels Management," PhD Thesis, Rensselaer Polytechnic Institute (1985).

9. "MCNP—A General Monte Carlo Code for Neutron and Photon Transport, Version 2B," LA-7396, Rev., Los Alamos National Laboratory (Apr. 1981).

10. M. S. MOORE and G. A. KEYWORTH, *Phys. Rev. C*, **3**, 1656 (1971).

11. M. R. BHAT, "Evaluation of ^{235}U Neutron Cross Section and Gamma Ray Production Data for ENDF/B-V," BNL-NCS-51184 (ENDF-248), Brookhaven National Laboratory (1980).

12. T. S. BELANOVA, A. G. KOLESOV, A. V. KLINOV, S. N. NIKOL'SKII, V. A. PORUCHIKOV, V. N. NEFEDOV, V. S. ARTAMONOV, R. N. IVANOV, and S. M. KALEBIN *Sov. At. Energy*, **47**, 772 (1979).

13. S. F. MUGHABGHAB, *Neutron Cross Sections, Vol. 1, Neutron Resonance Parameters and Thermal Cross Sections, Part B; Z = 61–000*, Academic Press, New York (1984).

14. R. W. BENJAMIN, K. W. MacMURDO, and J. D. SPENCER, *Nucl. Sci. Eng.*, **47**, 203 (1972).

15. H. DIAMOND, J. J. HINES, R. K. SJOBLOM, R. F. BARNES, D. N. METTA, J. L. LERNER, and P. R. FIELDS, *J. Inorg. Nucl. Chem.*, **30**, 2553 (1968).

16. K. W. MacMURDO and R. M. HARBOUR, *J. Inorg. Nucl. Chem.*, **34**, 449 (1972).

17. J. HALPERIN, G. D. O'KELLEY, J. H. OLIVER, J. E. BIGELOW, and J. T. WIGGINS, *Nucl. Sci. Eng.*, **90**, 298 (1985).

18. C. H. ICE, "Production of the Transplutonium Elements at Savannah River," Du Pont Savannah River Reports 66 through 69 (1966).

19. J. A. SMITH, C. J. BANICK, R. L. FOGER, and H. P. HOLCOMB, "Reactor Cross Sections for ^{242}Pu and ^{252}Cf," *Proc. 2nd Conf. Nuclear Cross-Sections and Technology*, Washington, D.C., March 4–7, 1968, Special Publication 299, Vol. II, p. 1285, National Bureau of Standards (1968).

20. J. HALPERIN, J. H. OLIVER, and P. W. STOUGHTON, "The Fission Thermal-Neutron Cross Section and Resonance Integral of ^{245}Cm, ^{247}Cm and ^{249}Cf," ORNL-4581, Oak Ridge National Laboratory (1970).

21. K. D. ZHURAVLEV, N. I. KROSHKIN, and A. P. CHETVEIKOV, *At. Energ.*, **39**, *4*, 285 (1975).

22. D. METTA, H. DIAMOND, R. F. BARNES, J. MILSTED, J. GRAY, Jr., D. J. HENDERSON, and C. M. STEVENS, *J. Inorg. Nucl. Chem.*, **27**, 33 (1964).

23. A. GILBERT and A. G. W. CAMERON, *Can. J. Phys.*, **43**, 1146 (1965).